

## A Cellular Automata Model of Oil–Water Partitioning

Chao-Kung Cheng

Department of Mathematical Sciences, Virginia Commonwealth University, Richmond, Virginia 23298

Lemont B. Kier\*

Department of Medicinal Chemistry, Virginia Commonwealth University, Richmond, Virginia 23298

Received February 13, 1995<sup>®</sup>

This study incorporates a gravity rule into the cellular automata modeling of two liquids and a solute. Beginning with a random mixture of these ingredients, the process of the formation of an immiscible system, a dynamic interface region, and the partitioning of the solute between the phases emerges. The dynamics reveal the formation of elongated aggregates or stacks of each liquid within the system. These stacks collect the solute to a degree commensurate with assigned rules. The stacks move toward the interface, producing a turbulent character. The partitioning process is seen in this model from a very early time in the dynamics.

### INTRODUCTION

The two-liquid system has aroused considerable interest for many years because of its ability to quantify solutes on the basis of their relative partitioning between them. This partitioning behavior has become identified with a number of biological phenomena such as drug absorption, protein binding, membrane passage, and some aspects of intermolecular interaction. This has led to the common practice of quantifying the propensity of a molecule to partition selectively between two immiscible liquids. This propensity, called lipophilicity, expressed quantitatively as the partition coefficient, has become a prominent entry in the rubric of properties of molecules, especially those of biological interest. Considerable effort has been made to identify the salient features of molecules that influence the partitioning between the liquids of immiscible systems. These reductionist approaches are conducted in an effort to model the property with a linear combination of information from these ingredients. We have asserted in our previous studies that water solutions and certainly a two-phase system with a solute are complex systems.<sup>1–4</sup> Understanding may then arise from dynamic synthesis of the emergent properties of these complex systems.

A number of studies have been reported on the mixing–demixing process using molecular dynamics and lattice models.<sup>5–9</sup> These begin with randomly distributed ingredients modeling members of a binary pair. Several computer simulations of the liquid–liquid interface have been reported. Simulations using Monte Carlo,<sup>10,11</sup> molecular dynamics,<sup>12,13</sup> and a lattice model<sup>14</sup> and a review<sup>15</sup> have focused attention on the interface structure of immiscible liquids. A recent molecular dynamics simulation by Benjamin<sup>16</sup> studied the water–dichloroethane interface. The ensuing dynamics develops the interfacial structure from an idealized origin. We would expect that an interface would evolve from a turbulent mixture of ingredients, as in the shake-flask experiments used to measure the partition coefficients of solutes. This expectation has guided us toward a model beginning with a heterogeneous random mixture of the two, ultimately immiscible liquids. As in our earlier studies,<sup>1–4</sup>

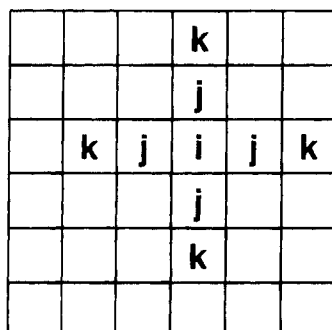


**Figure 1.** Extended von Neumann neighborhood of cell *i*.

we employ the dynamic simulation method of cellular automata.

### CELLULAR AUTOMATA

**The Model.** Cellular automata are dynamical systems that are discrete in space, time, and state and whose behavior is specified completely by rules governing local relationships. It is an attempt to simplify the often numerically intractable dynamic simulations into a set of simple rules that mirror intuition and that are easy to compute. As an approach to the modeling of emergent properties of complex systems it has a great benefit in being visually informative of the progress of dynamic events. From the early development by von Neumann,<sup>17</sup> a variety of applications ranging from gas phenomena to biological systems have been reported.<sup>18</sup> We have viewed cellular automata as an opportunity to advance our understanding of water and solution phenomena and have embarked upon a series of studies with this goal in mind.

Our model is composed of a grid of spaces called cells. Each cell *i* has four tesselated neighbors, *j*, and four extended neighbors, *k*, in what is called an extended von Neumann neighborhood (Figure 1). Each cell has a state governing whether it is empty or is occupied by a water or other molecule. The contents of a cell move, join with another occupied cell, or break from a tesselated relationship according to probabilistic rules generated as random numbers.

These rules are established at the beginning of each simulation. The rules are applied one after another to each

<sup>®</sup> Abstract published in *Advance ACS Abstracts*, November 1, 1995.

cell at random, the complete application of the rules to all cells constituting one iteration. The rules are applied uniformly to each cell and are local; thus there is no action at a distance. The cellular automata model is thus kinematic, asynchronous, and stochastic. The initial conditions are random; hence they do not determine the ultimate state of the cells, called the configuration. The same initial conditions do not yield the same set of configurations after any number of iterations except in some average sense. The configurations achieved after many iterations reach a collective organization that possesses a relative constancy in appearance and in reportable counts of attributes. What we observe and record from the cellular automata simulations are emergent attributes in a complex system.

**The Rules.** In previous reports we described the specifics of the calculations used.<sup>1-4</sup> We repeat these here in abbreviated form but include the new rules governing the gravity influence on the modeling of immiscible liquids. There are two kinds of cell occupants, active and boundary molecules. The active molecule can move so that the state of a cell occupied by an active molecule may change; however, a boundary molecule cannot move and thus the state of a cell occupied by a boundary molecule will not change. In this study, cells in two selected rows of the grid are occupied by boundary molecules. This transforms the torus model into a cylinder model. Those two rows, occupied with boundary molecules, serve as the top and the bottom of the cylinder. This introduces the notion of vertical direction to the model; therefore, a "gravity" attribute can be incorporated into the model.

Four parameters are adopted for our model to govern the probabilities for moving molecules in the grid. The breaking probability,  $P_B$ , used in our previous studies is the probability for an active molecule to break away from the molecule at  $j$  cells when there is exactly one occupied  $j$  cell (see Figure 1). The value for  $P_B$  lies in the closed unit interval. The second parameter,  $J$ , describes the movement of the active molecule at an  $i$  cell in the extended von Neumann neighborhood (Figure 1) when an adjacent intermediate  $j$  cell is vacant. It represents the ratio of the probability that a molecule at  $i$  cell will move toward an occupied  $k$  cell while the intermediate  $j$  cell is vacant, and the probability that a molecule at  $i$  cell will move toward a vacant  $k$  cell while the intermediate  $j$  cell is vacant.  $J$  is a positive real number. When  $J = 1$ , it indicates that the molecule  $i$  has the same probability of movement toward or away as for the case when  $k$  is empty. When  $J > 1$ , it indicates that  $i$  has a greater probability of movement toward an occupied  $k$  than when  $k$  is empty. When  $J < 1$ , it indicates that  $i$  has a lesser probability of movement toward  $k$  relative to when  $k$  is empty.

The third parameter,  $G_u$ , describes the movement of the active molecule at cell  $i$  relative to an active molecule in the  $j$  cell above it.  $G_u$  represents the ratio of the probability that an active molecule at  $i$  cell will switch places with the molecule in the  $j$  cell above it, and the probability that an active molecule at  $i$  cell will move toward a vacant  $k$  cell while the intermediate  $j$  cell is vacant.  $G_u$  is a nonnegative real number. When  $G_u = 1$ , it indicates that the active molecule  $i$  has the same probability to switch with the active molecule in the  $j$  cell above it as for the case when the molecule will move toward a vacant  $j$  cell when  $k$  is empty. The cases in which  $G_u > 1$  and  $G_u < 1$  have a similar specification. When  $G_u = 0$ , it indicates that switching is

**Table 1.** Iteration Time To Reach Equilibrium versus Temperature<sup>a</sup>

$P_B(W)$	$P_B(L_1)$	no. of $i(W)^b$	no. of $i(L_1)^c$
0.1	0.3	15000	5000
0.3	0.5	16000	14000
0.5	0.7	6000	5000
0.7	0.9	4000	3000

<sup>a</sup> Equilibrium assessed as relatively constant numbers of  $W$  in liquid phase and the numbers of liquid ( $L_1$ ) in the water phase. <sup>b</sup> Number of iterations to equilibrate water concentration in the liquid phase.

<sup>c</sup> Number of iterations to equilibrate the liquid concentration in the water phase.

not allowed with respect to the types of molecules involved. The fourth parameter,  $G_D$ , describes the movement of the active molecule at cell  $i$ , which switches cells with the active molecule in the  $j$  cell below it. This parameter is applicable only when the  $j$  cell below it is occupied with an active molecule. It represents the same information as  $G_u$  except this measures the switching probability with an active molecule below cell  $i$ .

At any iteration, the status of the dynamic simulation, referred to as the configuration, may be evaluated and recorded. In previous studies, we have utilized a number of these attributes to relate the simulations to physical reality. In addition, the graphic portrayal is available for observation after each iteration.

## AN IMMISCIBLE LIQUID SIMULATION

We have systematically studied and have optimized the choice of parameters for the simulation of an immiscible system. One ingredient is designated as water using the parameters established in earlier studies. For this study we use  $P_B(W) = 0.3$  and  $J(W) = 1$ . For the other liquid, we use  $P_B(L_1) = 0.5$  and  $J(L_1) = 0.5$ . For the cross-terms, we invoke a nonpolar character to the liquid  $L_1$  by using  $P_B(WL_1) = 0.9$  and  $J(WL_1) = 0.25$ . The gravity terms are  $G_D(WL_1) = 0.25$ ,  $G_u(WL_1) = 0.25$ ,  $G_D(L_1W) = 0.25$ , and  $G_u(WL_1) = 0.20$ . Thus, there is a modest preference for water to favor a position below the liquid  $L_1$  in a vertical encounter in the von Neumann neighborhood. The initial conditions are a random mix of 1050 water-occupied cells and 1050 liquid ( $L_1$ ) occupied cells in a grid of 3025 cells. We find that in the early stages of the dynamics, prior to the achievement of a stable configuration, there are formed isolated stacks of water cells above the interface and stacks of liquid cells below the interface (Figure 2). Figures 2 and 3 use parameter set one in Table 3. These gradually drift to the interface, forming connections with liquids of the same composition. At  $> 16\,000$  iterations, the fractions of water and liquid in their respective positions in the grid have become relatively stable. There is an increased concentration of each liquid in the other, near the interface. This is seen to be due to the presence of stacks of liquid cells arising from the bulk of each liquid, directed into the other liquid; see Figure 3. They move laterally and vertically as the dynamics proceeds.

These stacks are very similar to what others have described from dynamic simulations as capillaries<sup>10-14</sup> or fingers,<sup>16</sup> arising from each liquid and penetrating into the other phase. The stacks of liquid (capillaries) may extend into the other liquid by as much as 10 cells. Our simulation models the mixing and demixing phenomena of any two immiscible liquids since experimentally there is an inescapable amount



**Figure 2.** Configuration of immiscible liquids prior to the settling out into two phases. The water is black, the liquid is gray, and the cavities are white.



**Figure 3.** A configuration of immiscible liquids after a stable state has been achieved.

of turbulence at any newly formed interface that is going to produce some amount of heterogeneity. We should note, however, that the lack of direct knowledge about the structure of the interface and the difficulty of experimentally detecting the events is a situation facing investigators in this field.<sup>15</sup> The interface width has been defined as the span of space over which the water density has dropped from 90% to 10%

of its bulk value.<sup>11</sup> Various estimates of this dimension have been made from Monte Carlo and molecular dynamics simulations ranging from 5 to 10 Å. We find this dimension to be about 20 cells wide with a probable variation of 4 cells.

The influence of temperature on the formation and attributes of the interface have been simulated by varying the  $P_B(W)$  and  $P_B(L_1)$  values by 0.2 increment. We simulate

**Table 2.** Fractions of Water in Liquid Phase and Liquid in Water Phase at Equilibrium versus Temperature

$P_B(W)$	$P_B(L_1)$	$f(W)$	$f(L_1)$
0.1	0.3	0.35	0.40
0.3	0.5	0.10	0.22
0.5	0.7	0.12	0.20
0.7	0.9	0.17	0.23

**Table 3.** Partition Coefficients from Several Parameter Sets

no.	$P_B(WL_2)$	$P_B(L_1L_2)$	$P_B(L_2)$	partition coeff
1	0.7	0.3	0.7	4.0
2	0.7	0.3	0.3	3.0
3	0.7	0.7	0.3	2.0
4	0.7	0.7	0.7	1.3
5	0.3	0.3	0.3	1.0
6	0.3	0.3	0.7	0.9
7	0.3	0.7	0.7	0.3
8	0.3	0.7	0.3	0.3

a temperature range for this series of studies as shown in Table 1. Data were collected for the onset of the equilibrium value by counting the number of iterations to achieve a stable two-phase system. Table 1 reveals that over the range of parameters studied there is an optimum time to equilibrium when the  $P_B(W) = 0.3$  and  $P_B(L) = 0.5$ . When the system is warmer or cooler, the time to reach equilibrium is less. The influence of this same temperature change on the intersolubility of the liquids was also determined. The solubility is characterized by the count of cells of one liquid in the bulk domain of the other liquid at equilibrium. The dynamics, using four different sets of states for  $P_B(W)$  and  $P_B(L_1)$ , reveals a minimum solubility of the liquid in the water phase (Table 2). This minimum corresponds to the same set of probabilities giving rise to the optimum equilibrium time shown in Table 1. This agrees with the experimental observation that benzene exhibits a minimum solubility in water near room temperature.<sup>19,20</sup>

#### A MODEL OF PARTITIONING BETWEEN IMMISCIBLE LIQUIDS

With our dynamic model simulating some of the behavior of immiscible liquids, we can proceed to introduce a small number of solute molecules,  $L_2$ , to follow their partitioning behavior as a result of probabilistic rules. Using the optimized values of rules for W and  $L_1$ , described in the previous section, we have systematically varied the  $P_B$  rules governing the transitions,  $L_2L_2$ ,  $L_1L_2$ , and  $L_2W$ . These values are shown in Table 3. The initial conditions are 1000 cells occupied by water, 1000 cells occupied by liquid  $L_1$  and 100 cells occupied by solute  $L_2$ , all randomly scattered over the grid. We have elected not to use any gravity term relating  $L_2$  to W or  $L_1$ . Linse<sup>10</sup> addressed this issue and recognized the near negligible influence on molecules moving a few molecular diameters. The liquid phases were found to be stable after about 20000 iterations. Using the parameter combinations encoded in Table 3, we recorded the fraction of  $L_2$  solute molecules in the upper phase. The partition coefficient,  $P_C$ , is computed from  $P_C = [L_2]$  in the upper phase divided by  $[L_2]$  in the lower phase. It is assumed that delineation between the two phases is the middle row on the grid. About half of these parameter combinations in Table 3 produced results favoring the partitioning into the upper phase. The partition coefficient is influenced in these simulations primarily by the affinity of the solute for water,

$P_B(WL_2)$ . The numerical results are revealed from counts of molecules after certain numbers of iterations (Table 3).

A detailed description of how the partitioning process is occurring requires a continuous visual observation of the dynamics over an extended period of time. These observations have revealed an interesting and heretofore unrecorded prediction about what the sequence of events may be between a random mixture of solvents and solute, as in a shake-flask experiment, and the state of these three ingredients after partitioning has occurred. From a random initial state, the three ingredients move toward a configuration in which there are small stacks, of  $L_1$  in W and W in  $L_1$ . We show this configuration in Figure 4. We observe that the solutes,  $L_2$ , preferentially partition into  $L_1$  or W stacks, depending upon the parameters chosen. The stack favored is the same liquid phase in which the solute  $L_2$  is ultimately more concentrated. We can say that the partitioning process begins early with the appropriate liquid stack capturing many of the solute molecules well before an interface has formed. These stacks, one type with a significant concentration of solute  $L_2$  molecules, slowly move toward the now-forming interface (Figure 5). The stacks ultimately join with others to form the dynamic interface with the capillary structures, as we can see in Figure 6. The solute molecules,  $L_2$ , are now free to move through these capillaries and join the general concentration of solute in the bulk solvent. This sequence of events is depicted in the series of Figures 4–6 using parameter set 1 in Table 3.

#### DISCUSSION

The dynamic simulations described here reveal the formation of aggregates of identical cells that we call stacks. One type of stack, composed of either water or liquid, may have a preferential affinity for the solute molecules. These solute molecules are gathered up by the stacks in the early stages of the simulation. The stacks move toward the center of the grid and attach to the newly formed phase of the same type of liquid cells. The solutes are thus transported to the interface and ultimately to the phase in which they have an affinity. The ratio of concentrations of solute above and below the midline of the grid is taken to be the partition coefficient associated with that parameter set. Each parameter set characterizes the lipophilicity of that solute as we showed earlier.<sup>3</sup> The results of systematic variation in the parameter sets provide a useful profile of rule influence on the lipophilicity, as seen in Table 3. The dominant factor influencing the partition coefficient is the breaking probability of a water-solute pair encoded in  $P_B(WL_2)$ . When this value is high, describing a weak affinity between water and solute, we model a solute that is relatively nonpolar.<sup>3</sup> These solute molecules find their way predominately into the liquid phase representing the nonpolar or oil phase of the system  $L_1$ . When the water-solute ( $WL_2$ ) breaking probability is low, these two ingredients are similar and we conclude that the solute is relatively polar. In this case, the solute molecules prefer residency in the water phase and the partition coefficient is 1 or lower (Table 3). A secondary influence on the simulated partition coefficient comes from the breaking probability of the solute and the liquid  $P_B(L_1L_2)$ . Lower values of  $P_B(L_1L_2)$  within each subset of  $P_B(WL_2)$  values give higher partition coefficients. Thus a higher partition coefficient results from  $P_B(L_1L_2) = 0.3$  rather than

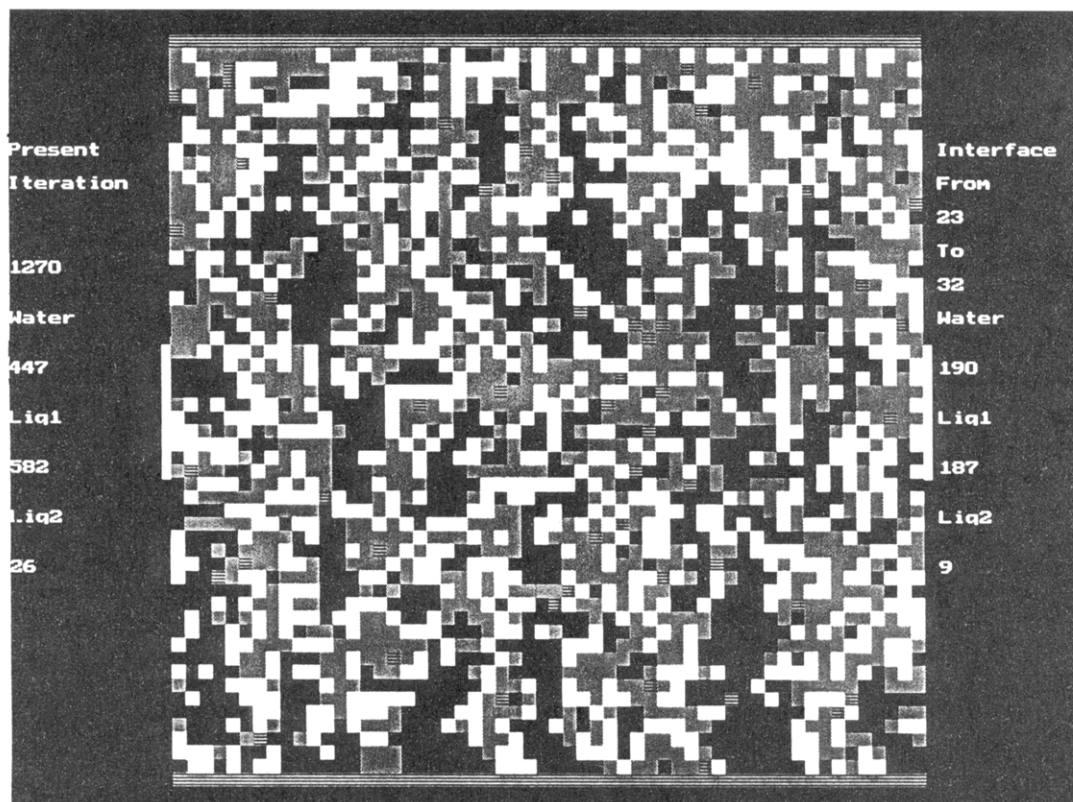


**Figure 4.** Configuration of two liquids and a solute shortly after random mixing. The solutes are the cross-hatched cells.



**Figure 5.** Configuration showing developed stacks of each liquid with one type predominantly capturing some solute molecules.

$P_B(L_1L_2) = 0.7$ , for a common value of  $P_B(WL_2)$ . Finally, the influence of the  $P_B(L_2)$  parameter is less than the other two breaking probabilities. The information from these comparative studies leads us to surmise that the dominant influence on partitioning or lipophilicity are the solute–solvent rules rather than the solute–solute rules. This is in line with a recent conclusion about solvent reorganization importance to the enthalpy of binding.<sup>21</sup>

The cellular automata dynamics described here portray a pair of immiscible liquids and a solute, organizing themselves into a relatively persistent configuration, identifiable as a partitioning phenomenon. This complex system and its emergent attributes arise from three rules, uniformly applied to each cell in its turn. The rules are probabilistic; hence the initial conditions influence each outcome only in an average sense. The dynamic simulation gives us an ever-changing

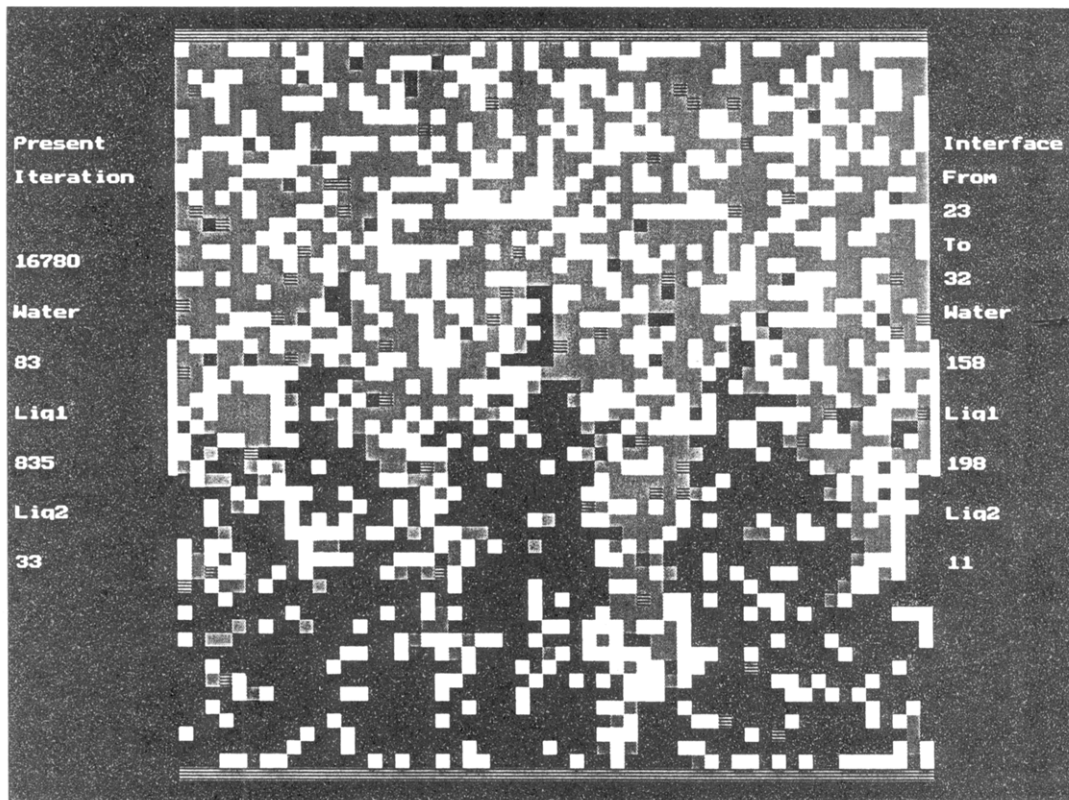


**Figure 6.** Stable interface showing partitioned distribution of solutes between the two liquids.

picture of events from the random distribution at the onset to the organized interface and solute distribution after many iterations. We configure the *process* rather than some frozen intermediate state, which certainly changes in the next time interval. Quantitative structure–activity analyses have been built around the capturing of frozen images, converting them into some quantitative parameter, and then finding a relationship with a property. This is useful, but is understanding developed to any extent? It is perhaps a new concept, to attempt to relate a property to an evanescent sequence, a process, a dynamic portrayal. This might be called a dynamic structure–activity model. Perhaps this and our earlier cellular automata simulations may provide an ingredient for such an approach.

#### ACKNOWLEDGMENT

L.B.K. thanks the A. D. Williams Foundation at Virginia Commonwealth University for a grant in support of this research. The dynamics were generated using the program DING-HAO.

#### REFERENCES AND NOTES

- (1) Kier, L. B.; Cheng, C.-K. A Cellular Automata Model of Water. *J. Chem. Inf. Comput. Sci.* **1994**, *34*, 647–652.
- (2) Kier, L. B.; Cheng, C.-K. A Cellular Automata Model of Aqueous Solution. *J. Chem. Inf. Comput. Sci.* **1994**, *34*, 1334–1337.
- (3) Kier, L. B.; Cheng, C.-K. A Cellular Automata Model of the Hydrophobic Effect. *Pharm. Res.* **1995**, *12*, 615–620.
- (4) Kier, L. B.; Cheng, C.-K. A Cellular Automata Model of Dissolution. *Pharm. Res.* **1995**, *12*, 1521–1525.
- (5) Nakaniishi, K.; Okazaki, S.; Ikari, K.; Higuchi, T.; Tawaka, H. Free Energy of Mixing, Phase Stability, and Local Composition in Lennard-Jones Liquid Mixtures. *J. Chem. Phys.* **1982**, *76*, 629–636.
- (6) Schoem, M.; Hoheisel, C. A Molecular Dynamics Simulation Study Using Lennard-Jones (12-6) Pair Potential Functions with Identical Sigma Parameters. *Mol. Phys.* **1984**, *53*, 1367–1380.
- (7) Malescia, G. Demixing and Mixing of Binary Hard-Core Yukawa Mixtures. *J. Chem. Phys.* **1992**, *82*, 1049–1062.
- (8) Scott, W.; Muller-Plathe, F.; Van Gunsteren, W. F. Molecular Dynamics Study of the Mixing and Demixing of a Binary Lennard-Jones Fluid. *Mol. Phys.* **1994**, *82*, 1049–1062.
- (9) Dijkstra, M.; Frenkel, D. Evidence for Entropy-Driven Demixing in Hard-Core Fluids. *Phys. Rev. Lett.* **1994**, *72*, 298–300.
- (10) Linse, P. Monte Carlo Simulation of Liquid–Liquid Benzene–Water Interface. *J. Chem. Phys.* **1987**, *86*, 4177–4187.
- (11) Gao, J.; Jorgensen, W. L. Theoretical Examination of Hexanol–Water Interfaces. *J. Chem. Phys.* **1988**, *92*, 5813–5822.
- (12) Meyer, M.; Mareschal, M.; Hayoun, M. Computer Modeling of a Liquid–Liquid Interface. *J. Chem. Phys.* **1988**, *89*, 1067–1073.
- (13) Carpenter, I. L.; Hehre, W. J. A Molecular Dynamics Study of the Hexane/Water Interface. *J. Phys. Chem.* **1990**, *94*, 531–536.
- (14) Smit, B.; Hilbers, P. A. J.; Esselink, K.; Rubert, L. A. M.; van Os, N. M.; Schlijper, A. G. Structure of a Water/Oil Interface in the Presence of Micelles: A Computer Simulation Study. *J. Phys. Chem.* **1991**, *95*, 6361–6368.
- (15) Hanna, G. J.; Noble, R. D. Measurement of Liquid–Liquid Interface Kinetics. *Chem. Rev.* **1985**, *85*, 583–598.
- (16) Benjamin, I. Theoretical Study of the Water/1,2-Dichloroethane Interface: Structure, Dynamics, and Conformational Equilibria at the Liquid–Liquid Interface. *J. Chem. Phys.* **1992**, *97*, 1432–1445.
- (17) von Neumann, J. In Theory of Self-Reproducing Automata; Burks, A., Ed.; University of Illinois Press: Urbana, IL, 1966.
- (18) Ermentrout, B.; Edelstein-Keshet, L. J. Cellular Automata Approaches to Biological Modeling. *Theor. Biol.* **1993**, *160*, 97–133.
- (19) Arnold, D. S.; Plank, C. A.; Erickson, E. E.; Pike, F. P. Solubility of Benzene. *Ind. Eng. Chem., Eng. Data Ser.* **1958**, *3*, 253–256.
- (20) Frank, F.; Gent, M.; Johnson, H. H. Solubility of Benzene in Water. *J. Chem. Soc.* **1963**, 2716–2720.
- (21) Cherenak, M. C.; Toone, E. J. A Direct Measure of the Contribution of Solvent Reorganization to the Enthalpy of Ligand Binding. *J. Am. Chem. Soc.* **1994**, *116*, 10533–10539.

CI950019Z